SAE International™

The Tire-Force Ellipse (Friction Ellipse) and Tire Characteristics

2011-01-0094
Published
04/12/2011

Raymond Brach
University of Notre Dame

Matthew Brach
Brach Engineering

Copyright © 2011 SAE International
doi:10.4271/2011-01-0094

ABSTRACT

The tire-force ellipse and tire-force circle (more frequently referred to as the friction ellipse and the friction circle, respectively) have been used for many years to qualitatively illustrate the concept of tire-road force interaction, particularly the force-limiting behavior for combined braking and steering (combined tire forces). Equations of the tire-force circle/ellipse, or, more specifically, the force limit envelope, in its idealized form have also been used in the development of quantitative models of combined tire forces used in vehicle dynamic simulation software. Comparisons of this idealized tire-force circle/ellipse using a simple bilinear tire force model and using actual tire data show that it provides only a limited, simplified notion of combined tire forces due to its lack of dependence upon the slip angle and traction slip. Furthermore, these comparisons show that the idealized tire-force circle/ellipse does not represent actual tire behavior, even approximately, since it is incapable of modeling the nonlinear behavior of tires. For this reason, the idealized tire-force circle/ellipse should not be used as a quantitative tire-force model particularly because superior validated models of nonlinear behavior of tires exist and are widely available. Here a development is presented of a more realistic version of the tire-force circle/ellipse which incorporates slip angle, traction slip and the actual nonlinear tire-force. Because of the complexity of nonlinear tire force behavior the F_y - F_x force relationship is not a true ellipse and the force limit is dependent on the kinematic slip angle and traction slip variables, α and s, respectively.

INTRODUCTION

The tire force developed over, and acting tangent to, the tire contact patch plane provides directional control of a vehicle as well as braking and acceleration traction. For analysis and modeling, this force is usually broken into its components, F_x and F_y. The former is the force component along the heading axis of the tire and supplies traction, whereas the latter is the force component perpendicular (normal) to the heading axis of the tire and controls steering. The resultant of these two forces is limited in magnitude by the tire characteristics, the tire-surface sliding friction and the normal force. Precipitated by friction concepts, the relationship of these two force components is often depicted as a circle or ellipse in (F_x, F_y) space. Often called a friction ellipse, it actually is a *tire-force ellipse*. Though not an exact ellipse, the force relationship in the mathematical form of an ellipse appears to be used for at least two purposes. The first is to portray the limit of the resultant of the tire force components, F_x and F_y, as the wheel slip and the slip angle change. A second purpose is to use the equation of the tire-force ellipse for modeling tire force components, particularly under the condition of combined braking and steering.

In general, it has been found that the longitudinal (traction) sliding friction coefficient, μ_x, and the lateral (steering) sliding friction coefficient, μ_y, for tires can differ. This effect is observable based on measurements of racing vehicles where lateral vehicle accelerations can exceed longitudinal accelerations. The threshold of the resultant tire force from control (partial slip) to sliding (full slip) varies with wheel slip, s, and slip angle, α. The limit of the resultant of the tire force components for any combination of s and α is μF_z, where μ is a combined sliding coefficient of friction and F_z is the normal force. If the friction coefficients for longitudinal sliding and lateral sliding are equal, the tire-force ellipse becomes a tire-force circle. In what follows, the term *tire-force circle* is used for brevity, but the results apply to a tire-force ellipse when $\mu_x \neq \mu_y$.

In addition to the tire force components, F_x and F_y, moments also develop over the contact area between a tire and the roadway. Although they form an important part of vehicle control, they are not discussed here. In practice, tire forces can be longitudinally and laterally asymmetrical [1]. Such asymmetry is also not discussed in the following. The term *adhesion* is often used in the tire literature to indicate non-slip of a tire over a portion of the tire-roadway contact region. In some cases it is even used synonymously with friction. However, current use of the term adhesion in the scientific literature refers to the presence of a tensile force over a contact area due to molecular attraction forces [2]. Since no significant tensile force is present between a tire and a road surface, this term is avoided herein. A detailed glossary of terms and acronyms is presented in the following section to provide consistent terminology within the paper.

A history of the friction circle is covered thoroughly in the book by Milliken and Milliken [8]. It should be pointed out that a related concept called the g-g diagram exists. The g-g diagram takes the form of the lateral acceleration of a vehicle (usually a racing vehicle) plotted versus its longitudinal acceleration as the vehicle undergoes cyclical motion (such as over a racing oval). Though similar in concept to a tire-force circle, the g-g diagram is a plot of *vehicle* kinematics and depends on vehicle effects (such as aerodynamics and suspension characteristics), not simply tire characteristics.

It is common practice to start an analysis of tire forces by relating the traction force component, F_x to the longitudinal slip, s and the lateral force component, F_y, to the slip angle, α. The relationship of the two force components is then established for combined braking and steering. This is the approach taken here. First, tire patch kinematics is covered. Experimental data are subsequently presented for use later in the paper to introduce the behavior of realistic tire force components, $F_y(\alpha)$ and $F_x(s)$. This is followed by presentation of an analytical model that allows the use of the components $F_y(\alpha)$ and $F_x(s)$ for a combined steering and traction force. Then the concept of the idealized tire-force circle is covered. Following that, the behavior of tire forces in $[F_y(\alpha,s), F_x(\alpha,s)]$ space, where α and s are parameters, is examined. Finally, the concept and use of the idealized tire-force circle for realistic tire behavior is examined. This paper is not intended to cover tire models. Discussions of the many models of tire forces can be found in the references in the paper by Sandu and Umrsrithong [12] and in the introduction of the papers by Brach and Brach [6, 7].

Properties and characteristics of the tire-force circle are examined for simple bilinear forms of the steering and traction components, F_y and F_x, and using the BNP tire force equations (Magic Formula) [3] with experimental data. In both cases, the tire forces for combined traction and steering are modeled using the Modified Nicolas-Comstock model [4, 5]. This model is chosen because of its efficiency and accuracy, but also because it can be used with any pair of traction and steering model equations.

Tire Kinematics

Two kinematic variables typically are used with tire force models and with the measurement of tire forces. These are the slip angle, α, and the longitudinal wheel slip, s. The slip angle is illustrated in Fig. 1 and is defined as

$$\alpha = \tan^{-1}(V_y / V_x) \tag{1}$$

The wheel slip can have different definitions [5]. The one used here is such that $0 \leq |s| \leq 1$ (for both positive and negative traction), where for braking

$$s = \frac{V_x - R\omega}{V_x} \tag{2}$$

Figures 1 and 2 show the tire slip velocity, V_P, has components $V_{Px} = V_x - R\omega$ and $V_{py} = V_y$. Note that, in general, the vector velocity, V, at the wheel hub and the slip velocity, V_p, at the contact patch center differ both in magnitude and direction. The slip velocity, V_p, is the velocity of a contact point P of the tire relative to the road surface.

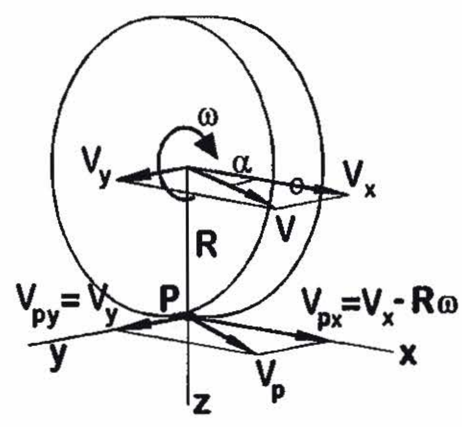

Figure 1. Wheel/tire velocity components

The directions of the resultant force, F, and the slip velocity, V_p, can differ. For no steering, ($\alpha = 0$) the longitudinal (traction) tire force component typically is expressed mathematically as a function of the wheel slip alone, $F_x(s)$. Similarly, for no braking, ($s = 0$), the lateral (cornering, steering) force component typically is expressed mathematically as a function of the sideslip angle alone, $F_y(\alpha)$.

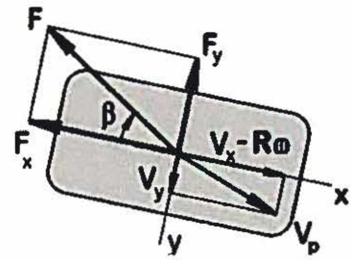

Figure 2. Tire patch velocity and force components.

Experimentally Measured Tire Forces

Experimental tire data is presented here because some of the results given later in the paper use tire parameters corresponding to values developed from these tests. One set of data used for illustrations in this paper is obtained from a cooperative research sponsored by NHTSA (National Highway Traffic Safety Administration) [10] for a 295/75R22.5 truck tire. Figure 3 shows the measured traction force $F_x(s)$ for different normal forces for zero slip angle, $\alpha = 0$. It shows that the slip stiffness, C_s, depends on the normal force. The slip angle stiffness coefficient, C_α (not shown), also depends on the normal force. Most importantly, the curves show that the longitudinal tire force, $F_x(s)$, over a large range of traction slip significantly exceeds the locked wheel force value $F_x(s)|_{s=1}$, at least for higher normal forces.

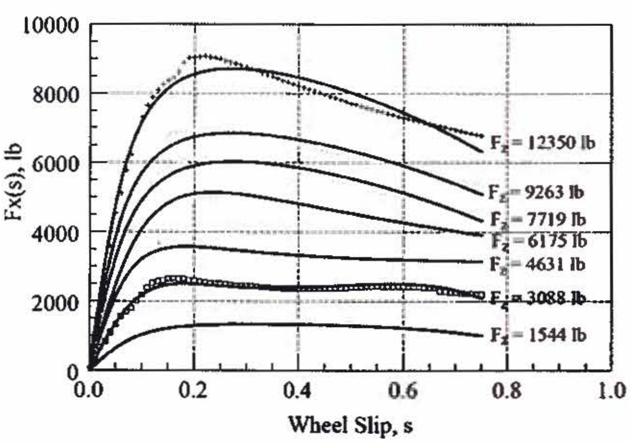

Figure 3. Measured traction forces [10] (symbols) for different normal forces, fitted by BNP model (solid curves).

Modified Nicolas-Comstock Model for Combined Steering and Traction

A mathematical model consisting of tire force equations for combined steering and traction, $F_y(\alpha,s)$ and $F_x(\alpha,s)$, for any given lateral force, $F_y(\alpha)$, and traction force, $F_x(s)$ expressions, has been established by Nicolas and Comstock [4] and modified by Brach and Brach [5]. Details of the modifications have been presented [6]. This model is referred to here as the MNC (Modified Nicolas-Comstock) model. In summary, equations of the combined tire forces are given as:

$$F_x(\alpha,s) = \frac{F_x(s)F_y(\alpha)s}{\sqrt{s^2F_y^2(\alpha)+F_x^2(s)\tan^2\alpha}} \times \frac{\sqrt{s^2C_\alpha^2+(1-|s|)^2\cos^2\alpha F_x^2(s)}}{sC_\alpha} \tag{3}$$

$$F_y(\alpha,s) = \frac{F_x(s)F_y(\alpha)\tan\alpha}{\sqrt{s^2F_y^2(\alpha)+F_x^2(s)\tan^2\alpha}} \times \frac{\sqrt{(1-|s|)^2\cos^2\alpha F_y^2(\alpha)+\sin^2\alpha C_s^2}}{C_s\sin\alpha} \tag{4}$$

The first quotient in Eq. 3 and in Eq. 4 is the original Nicolas-Comstock model equation and the second quotient is the correction factor. The accuracy and validity of these equations through comparison and contrast with other tire models has been presented [7]. Figure 3 shows an additional comparison using the truck tire data [10] fit using the BNP equations. Agreement between the curves generated by the BNP-MNC models and the experimental data illustrated in Fig. 4 is not perfect but reasonably good. Agreement is best for lower levels of braking, that is, lower levels of $F_x(\alpha,s)$. Agreement is not as good for higher levels of $F_x(\alpha,s)$. Trends of the modeled tire forces and the shapes of the combined tire-force curves all are appropriate. Regardless, it is quite apparent that the idealized tire-force circle (shown in Fig. 4 with a dashed line) is not a good predictor of the data and that the MNC model does a better job at approximating the data.

A unique feature of the MNC theory is that it consists of continuous analytical equations and can be used with any steering and traction equations, $F_y(\alpha)$ and $F_x(s)$. This is exploited in following sections.

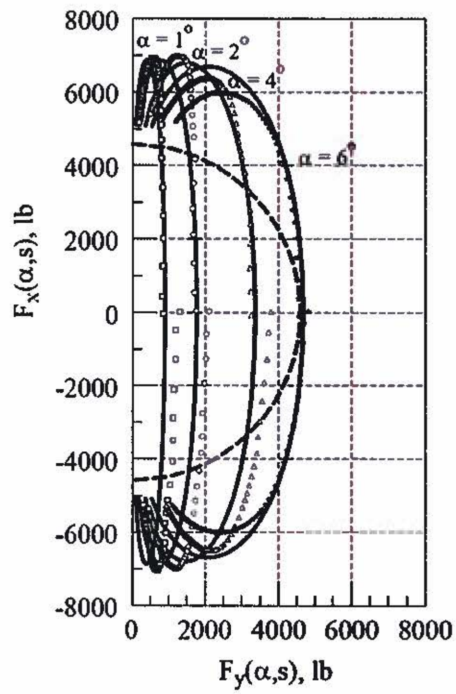

Figure 4. Tire data [10] (symbols) compared to the combined BNP-MNC model (solid curves) for a normal force of F_z = 9263 lb. The dashed curve is the idealized tire-force circle.

The (Idealized) Tire-Force Circle

Before comparing different tire models and tire data to the tire-force circle, it is useful to look quantitatively at the concept. The tire-force circle typically is used to portray limiting tire-force behavior. An expression for the equation of the tire-force circle can be developed based on the tire forces at the patch $F_x(\alpha,s)$, $F_y(\alpha,s)$, F_z, and the coefficients of friction, μ_x and μ_y. Similar concepts have been developed and presented elsewhere [8, 9].

Using the fundamental equation of an ellipse with the major axis equal to $2\mu_x F_z$, the minor axis equal to $2\mu_y F_z$, the horizontal variable equal to $F_y(\alpha,s)$ and the vertical variable equal to $F_x(\alpha,s)$ is:

$$\frac{F_y^2(\alpha,s)}{\mu_y^2 F_z^2} + \frac{F_x^2(\alpha,s)}{\mu_x^2 F_z^2} \le 1 \tag{5}$$

The inequality in Eq. 5 indicates that as long as the resultant force remains inside the tire-force circle, skidding (full sliding) does not occur and steering control is maintained. Equality in Eq. 5 corresponds to full sliding, for example, when the wheel slip, $s = 1$ for any α or $\alpha = \pi/2$ for any s. Under these conditions, the direction of the resultant force, F, opposes the velocity; $\beta_F = \alpha$, $F_x = -F\cos\alpha$, $F_y = -F\sin\alpha$ (see Fig. 2) and

$$\frac{F^2\sin^2\alpha}{\mu_y^2 F_z^2} + \frac{F^2\cos^2\alpha}{\mu_x^2 F_z^2} = 1 \tag{6}$$

When $\mu_x = \mu_y$, this is the equation for a circle as shown in Figure 4. During sliding, $F = \mu F_z$, then Eq. 6 can be written as

$$\frac{\sin^2\alpha}{\mu_y^2} + \frac{\cos^2\alpha}{\mu_x^2} = \frac{1}{\mu^2} \tag{7}$$

Simplification yields:

$$\mu^2 = \frac{\mu_x^2\mu_y^2}{\mu_y^2\cos^2\alpha + \mu_x^2\sin^2\alpha} \tag{8}$$

and, taking the square root of both sides gives:

$$\mu = \frac{\mu_x\mu_y}{\sqrt{\mu_x^2\sin^2\alpha + \mu_y^2\cos^2\alpha}} \tag{9}$$

Equation 9 permits a combined coefficient of sliding friction to be determined for any combination of μ_x, μ_y and α. The sliding friction force, μF_z, can then be determined for a given value of F_z; Equation 9 reduces to an identity for $\mu_x = \mu_y$. These equations illustrate the concept of an idealized tire-force circle whereby it illustrates the limit of directional control (inside the circle) and full sliding when the resultant tire force reaches the circle.

The above describes how the tire-force circle is used as a quantitative description of the limiting behavior of the resultant tire force due to friction. The tire-force circle equations are also used in some simulation software programs [7] in the following manner. A constant level of braking force is specified, that is, $F_x(\alpha,s) = F_B$. Then Eq. 5, using the equality sign, is used to solve for a corresponding steering force such that

$$F_y(\alpha,s) = \mu_y F_z \sqrt{1 - \frac{F_B^2}{\mu_x^2 F_z^2}}$$

(10)

If $F_B = \mu_x F_z$, then $F_y = 0$. If $F_B < \mu_x F_z$, then $F_y > 0$ and a steering force component is available for directional control. For full sliding, $F_x = \mu_x F_z \cos\alpha$ and $F_y = \mu_y F_z \sin\alpha$. These conditions place the steering and traction forces on the tire-force circle whose magnitude is limited by the sliding friction coefficients. As already seen from Fig. 4 tire forces can exceed the limits predicted by the idealized tire-force circle by significant amounts. Consequently, the use of Eq. 10 as a tire-force model is unrealistic. This is examined below in more detail.

Bilinear Steering and Traction Force Models

The first examination of the tire-force circle concept is for simple, bilinear force curves which are often used as a simple tire model in simulation software [6, 7]. That is,

$$F_y(\alpha) = \begin{cases} C_\alpha \alpha, & 0 \le \alpha \le \alpha_1 \\ \mu_y F_z, & \alpha_1 < \alpha \le \pi/2 \end{cases}$$

(11)

where C_α is the lateral stiffness coefficient of the tire and $\alpha_1 = \mu_y F_z / C_\alpha$. The longitudinal force is given by:

$$F_x(s) = \begin{cases} C_s s, & 0 \le s \le s_1 \\ \mu_x F_z, & s_1 \le s \le 1 \end{cases}$$

(12)

where C_s is the traction stiffness coefficient and $s_1 = \mu_x F_z / C_s$. If Eqs. 11 and 12 are placed into the MNC equations, it is possible to illustrate the variation of $F_y(\alpha,s)$ with respect to $F_x(\alpha,s)$. Figures 5 and 6 are examples. Figure 5 shows the force component relationship for selected, constant wheel slip values and varying slip angles. Figure 6 shows the force component relationship for selected, constant values of the slip angle and varying longitudinal slip.

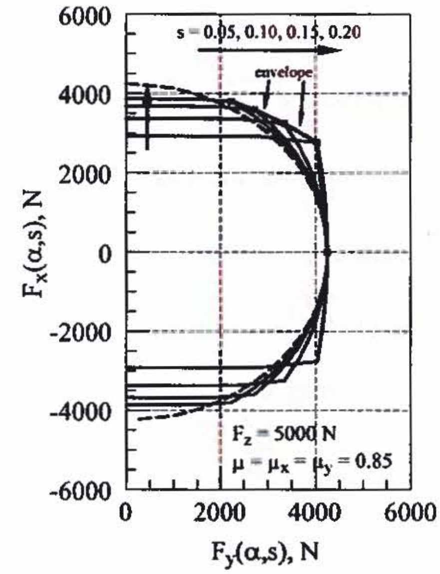

Figure 5. Dashed curve is the idealized tire-force circle and solid curves are from the bilinear tire-force curves for constant s, generated by the MNC model.

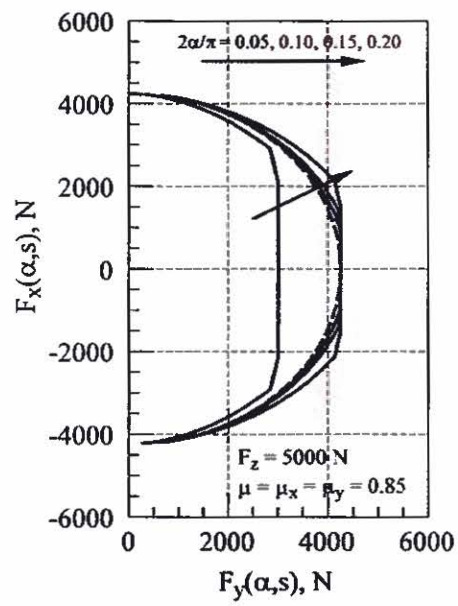

Figure 6. Dashed curve is the idealized tire-force circle and solid curves are from the bilinear tire-force model for constant α, generated by the MNC model.

Experimental Tire-Force Models (BNP)

Rather than simple bilinear force relationships, tire forces are developed using the BNP model fitted to experimental data [11]. The Appendix shows specific $F_y(\alpha)$ and $F_x(s)$ curves obtained from fitting the BNP equations for a P225/60R16 tire. These can be placed into the MNC combined steering and traction equations to generate the tire force envelopes shown in Figs. 7 and 8. These curves have one characteristic in common with the curves derived from bilinear relationships in Fig. 5 and 6, namely that significant portions of the combined force exist outside of the idealized tire-force circle. Beyond that similarity, the shape of the curves differs from those generated from the bilinear tire force model significantly. In particular, Figs. 7 and 8 show that significant portions of both the steering and traction forces lie further outside of the idealized tire-force circle (shown with a dashed curve).

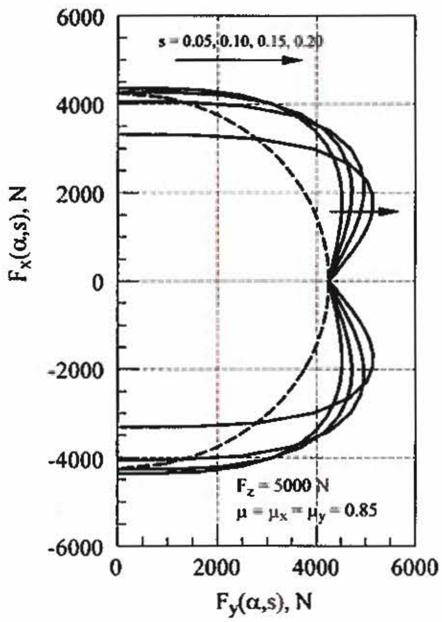

Figure 7. Dashed curve is the idealized tire-force circle and solid curves are from BNP tire force curves based on experimental data [11] for constant values of s, generated by the MNC model.

In order to illustrate actual combined tire force levels that exist outside of the idealized tire-force circle, a single curve comparable to Figs. 7 and 8 was generated by sampling values of $F_y(\alpha, s)$ and $F_x(\alpha, s)$ for $0 \le s \le 1$ and $0 \le 2\alpha/\pi \le 1$ using the MNC equations. This selection was carried out using the Monte Carlo technique with no statistical relationship between α and s intended. The result is shown in Fig. 9. It shows the existence of a limit curve, shown dashed. It does not have the exact shape of a circle but is roughly circular in nature. The idealized tire force circle (inner curve, Fig 9) might be considered as a conservative estimate of the tire force limit curve but for a full range of slip values, α and s, it can be quite inaccurate.

It can be noted that the spacing is relatively large between the constant-α curves in Fig. 6 and 8 when the slip angle is small and decreases dramatically for larger values of α. This is because of the rapid change of the lateral force for small slip angle, α, to an almost constant value for larger values (for example, see Fig. 3).

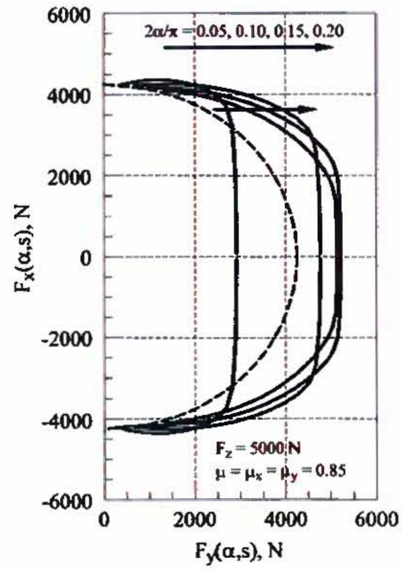

Figure 8. Dashed curve is the idealized tire-force circle and solid curves are from BNP tire force curves based on experimental data [11] for constant values of α, generated by the MNC model.

Tire-Force Circle (Ellipse)

At this point the concept (and utility) of a tire-force circle, or ellipse, can be examined. It is apparent from the examination of the tire-force curves above (Figs. 5, 6, 7, and 8) that the idealized tire-force circle cannot be used to characterize the behavior of real tires, especially the limiting behavior due to friction. This disparity in the characterization of performance raises the question, what is the definition of the tire-force circle? One definition could be that it is the envelope of the maximum force that can be developed by a tire for all values of slip angle, α and wheel slip s. For example, Fig. 9 shows such an envelope. Each of the points surrounded by the envelope corresponds to different values of α and s. This is also apparent from the MNC equations, Eq. 3 and 4. All of the tire-force curves (Figs. 5, 6, 7, 8, and 9) are plots of the tire force component in $[F_y(\alpha,s), F_x(\alpha,s)]$ space. If Eq. 4 is divided by Eq. 3, the slope of the curves in $[F_y(\alpha,s), F_x(\alpha,s)]$ space is obtained, including the friction limits. It is clear that the slopes are functions of α and s. Consequently the envelope is a function of α and s.

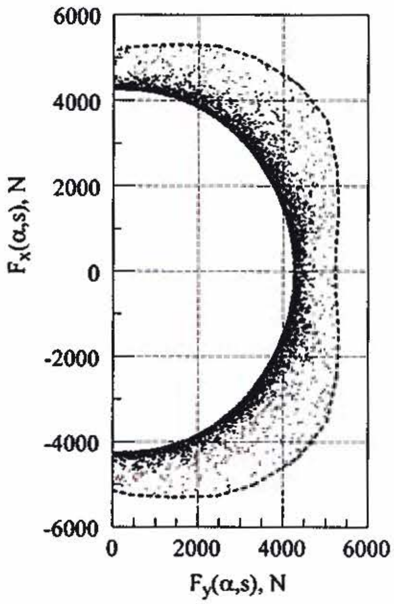

Figure 9. Tire-force values indicated by dots outside of the idealized tire-force circle (dark, inner curve) are those from the BNP equations and MNC equations (F_z = 4250 N). A realistic force limit is shown by the dashed curve.

SUMMARY/CONCLUSIONS

In summary, the BNP-MNC tire model equations have been shown to be a reasonably accurate tire model for the combined steering and braking force components, $F_y(\alpha,s)$ and $F_x(\alpha,s)$, over the full range of the slip variables, $0 \leq \alpha \leq \pi/2$ and $0 \leq s \leq 1$. This accuracy was demonstrated in previous papers [5, 6, 7] with additional validation provided in this paper. Once the validity of BNP-MNC tire model over the full range of independent variables was established, it then was used as a tool to investigate how well the idealized tire-force ellipse (friction ellipse) predicts the limit of the tire forces, $F_y(\alpha,s)$ and $F_x(\alpha,s)$, as a tire transitions from slip to full sliding over the full range of independent variables α and s. The analysis shows that the idealized tire-force ellipse does not accurately describe the limits of the combined tire forces. In general, it significantly underpredicts the limiting force and consequently cannot be used qualitatively to describe tire force limits. Furthermore, since the idealized tire-force ellipse does not accurately describe the force limits of a tire, it cannot accurately serve as a quantitative, mathematical model for the calculation of tire forces.

The BNP equations coupled with the MNC equation provide a means to study the behavior of tire forces under combined steering and traction. Figure 4 shows that the BNP-MNC equations reasonably represent the behavior of tire forces. For tire forces in the range of routine driving (moderate braking and low front wheel steering angles) Fig. 10 shows the central portion of Fig. 4 and illustrates that the BNP-MNC model equations are accurate in this range.

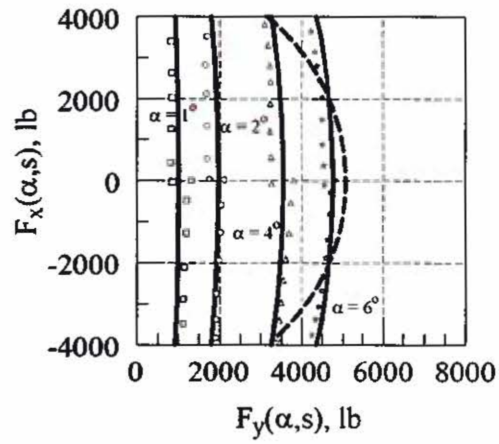

Figure 10. Central portion of Fig. 4 showing the range of steering and and traction forces for moderate steering and braking.

When the traction forces are relatively high, such as for emergency braking, Fig. 11 shows that the BNP-MNC model equations are less accurate but do follow the trends of the combined tire force behavior. A reason for the departure of the model and data is likely due to the large, nonlinear lateral and circumferential elastic deformations of the tire when testing and operating under these conditions.

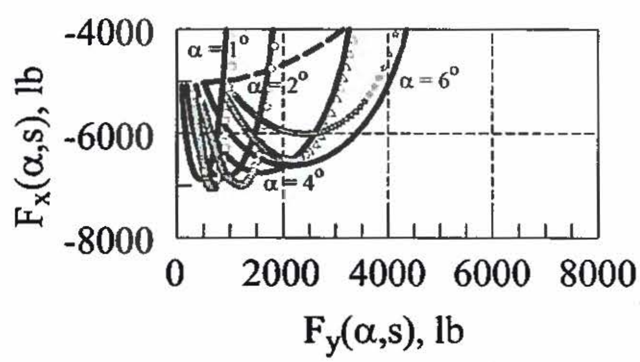

Figure 11. Portion of Fig. 4 showing the region of combined tire forces for heavy braking.

The concept of the idealized tire-force circle/ellipse (friction ellipse) serves as a rough qualitative way of explaining how the resultant tire force is limited by sliding friction, but the equations of the circle provide inaccurate quantitative information. The idealized tire-force circle/ellipse should never be used as a tire force model because it provides unrealistic and significantly low values of tire forces over a wide range of slip values, perhaps with the exception of a tire operating in linear slip ranges of α and s (that is, when $F_y(\alpha)$

$\sim C_\alpha \alpha$ and $F_x(s) \sim C_s S$). The main reason that the idealized tire-force circle is inaccurate is because $F_y(\alpha)$ and $F_x(s)$ individually can exceed the sliding value, μF_Z, over significant ranges of the slip values as determined experimentally (see Fig. 3). Using the BNP-MNC model equations, Figs. 7 and 8 show that the idealized tire-force circle can underpredict the resultant force even when the maximum values of $F_y(\alpha)$ and $F_x(s)$ each are less than or equal to μF_z. It is not possible to improve the concept of the idealized tire-force circle/ellipse (friction ellipse) for use as a tire model because it is independent of the slip variables, α and s, and because a linear model does not adequately represent the nonlinear behavior of tire forces.

A major goal of this paper is to show, as illustrated in Fig. 9, that a universal tire-force limit, or envelope, is significantly larger than predicted by the idealized tire-force ellipse and to show that the limit curve is dependent on α and s. This was done using the BNP-MNC model since it is adaptable to any set of functions, $F_y(\alpha)$ and $F_x(s)$.

REFERENCES

1. Pottinger, M. G., "Tire Force and Moment in the Torqued State and Application of the Flat-Trac II Tire Test Machine", Clemson Tire Conference, Greenville, SC, October 1990.

2. Cheng, W., Dunn, P. F. and Brach, R. M., "Surface Roughness Effects on Microparticle Adhesion", *J. Adhesion*, 78, 2002, 929-965.

3. Bakker, E., Nyborg, L., and Pacejka, H.B., "Tyre Modeling for Use in Vehicle Dynamic Studies," SAE Technical Paper 870421, 1987, doi: 10.4271/870421.

4. Nicolas, V. T. and Comstock, T. R., "Predicting Directional Behavior of Tractor Semitrailers When Wheel Anti-Skid Brake Systems Are Used", Paper No. 72 - WA/ Aut-16, ASME Winter Annual Meeting, November 26-30, 1972.

5. Brach, R.M. and Brach, R.M., "Modeling the Combined Braking and Steering Forces," SAE Technical Paper 2000-01-0357, 2000, doi: 10.4271/2000-01-0357.

6. Brach, Raymond and Brach, Matthew, "Tire Models used in Accident Reconstruction Vehicle Motion Simulation", XVII Europäischen Vereinigung für Unfallforschung und Unfallanalyse (EVU) - Conference, Nice, France, 2008.

7. Brach, R.M. and Brach, R.M., "Tire Models for Vehicle Dynamic Simulation and Accident Reconstruction," SAE Technical Paper 2009-01-0102, 2009, doi: 10.4271/2009-01-0102.

8. Milliken, W.F. and Milliken, D.L., "Race Car Vehicle Dynamics," SAE International, Warrendale, PA, ISBN 978-1-56091-526-3, 1994.

9. Wong, J. Y., *Theory of Ground Vehicles*, John Wiley and Sons, Inc, 1993.

10. "Statement of Work, Truck Tire Characterization Phase 1 Part 2, Cooperative Research," Funding by NHTSA, Contract No. DTNH22-92-C-17189, SAE International, Warrendale, PA 1995.

11. Salaani, M.K., "Analytical Tire Forces and Moments Model with Validated Data," SAE Technical Paper 2007-01-0816, 2007, doi:10.4271/2007-01-0816.

12. Umsrithong, A. and Sandu, C., "A Semi-Empirical Tire Model for Transient Maneuver of On Road Vehicle," SAE Technical Paper 2009-01-2919, 2009, doi: 10.4271/2009-01-2919.

Notation, Acronyms and Definitions

BNP

Bakker-Nyborg-Pajecka equations (also known as the Magic Formula) [3]

cornering stiffness

see C_α

frictional drag coefficient

average, constant value of the coefficient of friction of a tire fully sliding over a surface under given conditions (wet, dry, asphalt, concrete, gravel, ice, etc.) appropriate to an application

friction circle

see tire-force circle

full sliding

a condition when the combined slip variables (α, s) give a resultant tire force equal to μF_z

g-g diagram

a plot of the lateral acceleration of a vehicle versus its longitudinal acceleration

lateral (side, cornering, steering)

in the direction of the y axis of a tire's coordinate system,

longitudinal (forward, rearward, braking, accelerating, driving)

in the direction of the x axis of a tire's coordinate system

longitudinal stiffness

see C_s

MNC
: Modified Nicolas-Comstock equations [4, 5]

sideslip
: see slip angle

sliding
: the condition of a wheel moving over a roadway surface locked from rotating ($s = 1$), or moving sideways ($\alpha = \pi/2$)

slip velocity
: the velocity relative to the ground of the center of a wheel at the contact patch (see V_P, Fig. 2),

slip angle
: the angle, α, between the direction of the velocity of a wheel's center (hub) and the wheel's heading axis (see Fig. 1)

tire-force circle; tire-force ellipse
: an idealized curve with coordinate axes consisting of the lateral and longitudinal tire force components, $F_y(\alpha,s)$ and $F_x(\alpha,s)$, that qualitatively relates the behavior of the resultant tire force over the full range of kinematic variables, α and s

traction
: the term traction is used to indicate a longitudinal force, either acceleration or braking

wheel slip
: a kinematic variable, s, ranging between 0 and 1 that quantifies the longitudinal motion of the wheel relative to the road surface

C_α
: lateral tire force coefficient (also cornering coefficient)

C_s
: tire force traction coefficient, the rate of change of the traction force at zero slip, s

$F_x(s)$
: an equation with a single independent variable, s, that models a longitudinal tire force *for no steering, $\alpha = 0$*

$F_y(\alpha)$
: an equation with a single independent variable, α, that models a lateral force *for no braking, $s = 0$*

$F_x(\alpha,s) \equiv F_x[F_x(s),F_y(\alpha),\alpha,s]$
: an equation with two independent variables, α and s, that models a longitudinal tire force component *for combined braking and steering*

$F_y(\alpha,s) \equiv F_y[F_x(s),F_y(\alpha),\alpha,s]$
: an equation of two independent variables, α and s, that models a lateral tire force component *for combined braking and steering*

F_z
: wheel normal tire force

V_x, V_y
: components of the velocity of a wheel's hub expressed in the tire's coordinate system

V_P
: slip velocity of a tire at point P of the tire patch (see Fig. 2)

x-y-z
: orthogonal tire coordinates where x is in the direction of the wheel's heading and z is perpendicular to the tire's contact patch

α
: tire slip angle (also, tire sideslip angle and lateral sideslip angle)

β_P
: angle of a tire's slip velocity relative to the tire's x axis and angle of the resultant force parallel to the road plane

μ_x
: tire-surface frictional drag coefficient measured for full sliding in the longitudinal direction, $s = 1$, $\alpha = 0$

μ_y
: tire-surface frictional drag coefficient measured for full sliding in the lateral direction, $\alpha = \pi/2$

APPENDIX

BNP Equations and Constants

Data from Salaani [11] were used to provide a comparison of actual tire force behavior to the idealized tire-force circle. Data from $F_y(\alpha)$ and $F_x(s)$ measurements were each fit to the BNP equations and scaled to a common normal force values (steering measurements and traction measurements were not made at exactly 5000 N). These BNP equations then were placed into the MNC equations to provide $F_y(\alpha,s)$ and $F_x(\alpha,s)$ functions. A range of specific values of s and α were used to compute the corresponding curves plotted in Figs. 7 and 8. The BNP equations [3] can be written as:

$$P(u) = D\sin[C\tan^{-1}(B\phi)] \tag{A1}$$

where

$$\phi = (1-E)Ku + (E/B)\tan^{-1}(BKu) \tag{A2}$$

For example, Fig. A-1 shows the measured and BNP least-square fitted values for the measurements of $F_x(s)$ and Fig. A-2 shows the corresponding fit of $F_y(\alpha)$ data.

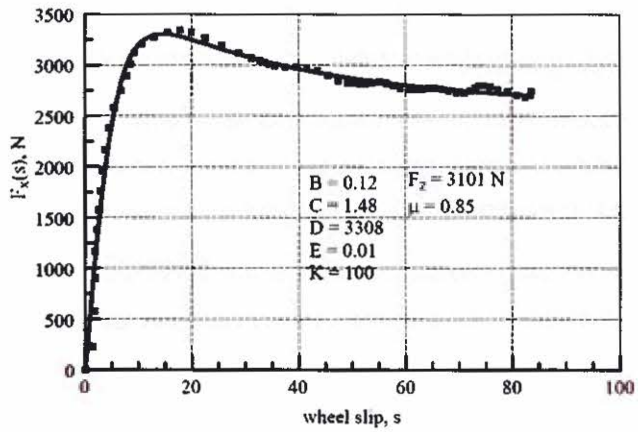

Figure A-1. Solid line is a BNP curve fit to traction data from a test of a P225/60R16 tire [4]. Values of the BNP constants are shown.

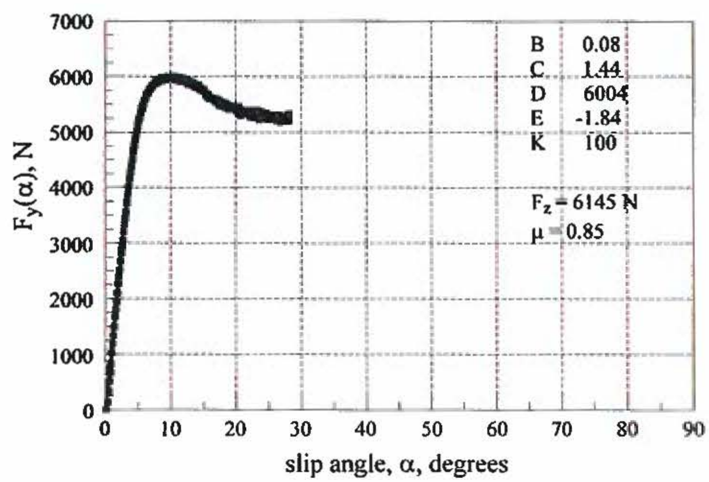

Figure A-2. Solid line is a BNP curve fit to steering data from a test of a P226/60R16 tire [4]. Values of the BNP constants are shown.

The Engineering Meetings Board has approved this paper for publication. It has successfully completed SAE's peer review process under the supervision of the session organizer. This process requires a minimum of three (3) reviews by industry experts.

All rights reserved. No part of this publication may be reproduced, stored in a retrieval system, or transmitted, in any form or by any means, electronic, mechanical, photocopying, recording, or otherwise, without the prior written permission of SAE.

ISSN 0148-7191

Positions and opinions advanced in this paper are those of the author(s) and not necessarily those of SAE. The author is solely responsible for the content of the paper.

SAE Customer Service:
Tel: 877-606-7323 (inside USA and Canada)
Tel: 724-776-4970 (outside USA)
Fax: 724-776-0790
Email: CustomerService@sae.org
SAE Web Address: http://www.sae.org
Printed in USA

SAE International